ISSN: 0067-2904

Characterization of Ag:Ni Nano Particles Produced by Pulse Nd:YAG laser

Ahmed Abd Al-Razza Naama
Department of Physics, College of Science, University of Baghdad, Baghdad, Iraq.

Abstract

This work presents the characteristics of plasma produced by fundamental wavelength (1064 nm) Q- switched Nd:YAG laser on Ag:Ni alloy in distilled water were investigated at different laser energies by optical emission spectroscopy technique. The size of produced nanoparticles from Ag:Ni target in distilled water were studied, by x-ray diffraction, UV-visible absorbance and atomic force microscopy, at different laser energies. Spectroscopic measurements show that electron temperature and electron density increase with increasing laser energy. It was found from AFM measurements that the produced nanoparticle size decrease from 97.13 nm to 71.20 nm, while XRD shows that the crestalline size decrease from 15.5 nm to 9 nm with increasing pulse laser energy. UV- visible absorbance shows at plasmon peaks shifted from 410 to 395 nm with increasing laser energy.

Keywords: Plasmon; Ag:Ni nanoparticles, X-ray diffraction .

تشخيص دقائق Ag:Ni النانوية المنتجة بواسطة ليزر النيوديميوم–ياك النبضي

أحمد عبد الرزاق نعمة
قسم الفيزياء، كلية العلوم، جامعة بغداد، بغداد، العراق.

الخلاصه

هذا البحث هو دراسة لخصائص البلازما المنتجة عن طريق الليزر النبضي ذو محول عامل النوعية نيوديوم ياك (Nd:YAG) من سبيكة Ag: Ni في الماء المقطر عند طاقات مختلفة لليزر بواسطة تقنية التحليل الطيفي للانبعاثات. تم دراسة تأثير الطاقات المختلفة لليزر على الحجم االنانوي للدقائق المنتجة من هدف Ag:Ni في الماء المقطر باستخدام حيود الاشعة السينية و امتصاص الاشعة المرئية فوق البنفسجية ومجهر القوى الجزيئية. تبين من القياسات AFM أن حجم الجسيمات النانوية ينخفض من 97.13 إلى 71.20 نانومتر ، بينما أظهرت قياسات XRD انخفاض الحجم البلوري من 15.5 نانومتر إلى 9 نانومتر مع زيادة طاقة الليزر النبضي. يظهر طيف امتصاص الأشعة فوق البنفسجية– مرئية قمة البلازمون تزحزحت 410–395 نانومتر مع زيادة طاقة الليزر.

Introduction

Metal nanoparticles are sure to be the building unit of the up and coming era of electronic and sensors [1]. The metal nanoparticles, are exceptionally among a nanomaterial due to their physical and concoction properties and to their many applications [2]. metals like gold and silver began to be seriously concentrated on in the most recent decades, in view of their remarkable properties which

Email: ahmaddualah@yahoo.com

make them valuable for applications in a few quickly creating fields like photonics, disease treatment and in vivo Raman spectroscopy [3].

There are many techniques to fabricate metal nanoparticles or alloys, such as exploding wire[4], chemical bath [5] and pulsed laser deposition [6] etc. Pulsed laser deposition use as a noble technique for the nanostructures fabrication of various materials because of its talent to control the size and shape of Nano-materials by adjusting the laser parameters, the surrounded material, target property[7]. Pulsed laser-induced plasmas spectroscopy (LIPS) of alloys have more attention for used in several applications [8]. Light emitted from the plasma generated by high- power laser pulses were analyzed and the spectrum often consists of a number of characteristic spectral lines of a particular atoms or ions. Plasma temperature calculated using Boltzmann relation [9]

$$Ln\left(\frac{I_{mn}\lambda_{mn}}{g_m A_{mn}}\right) = \left(\frac{E_m}{KT_e}\right) + \left(\frac{N(T)}{U(T)}\right) \quad (1)$$

where λ_{mn}, I_{mn}, g_m, and A_{mn} are the wavelength, intensity, statistical weight, and transition probability between the transition states of upper to lower levels (m→ n).

The electron density was calculated using Saha-Boltzmann equation for atomic and ionic spectral lines [10].

$$n_e = \frac{2(2\pi m_e kT)^{3/2}}{h^3} \frac{I^I_{mn} A_{jk} g^{II}_j}{I^{II}_{jk} A_{mn} g^I_m} e^{-(E_{ion}+E^{II}_j - E^I_m)/kT} \quad (2)$$

where E_{ion} is the ionization energy, E_m and E_j are the upper level energies of neutral and single ionized transitions.

Plasmon is a dipole electron oscillations limited by particles wall in Nano scale when the a specific frequency of incident light scattered with metal nanoparticles or thin Nano metallic layers with sub wavelength scale [11].

Experimental Part

Ag:Ni alloy was prepared using equal quantities of silver and nickel powders (99.99% purity from Ossila company - UK) and mix them by mechanical motor with steel balls for 10 minutes. A piston under a pressure of 3.5 tons was used to make a pellet of 1 gm 0.9 cm diameter and 0.3 cm thickness.

The target samples were put in the bottom of 5 ml quartz tube filled with distilled water then bombarded by Nd:YAG pulse laser (Hua Fei Tong Da Technology –Diamond -288 Pattern EPLS) at 6 Hz frequency and 9 ns pulse duration with 1064 nm wavelengths and with several pulse energies (300, 400, 500, 600, 700 and 800) mJ, the selection of these energies as their spectral lines can be distinguished by spectroscopy.

The emission of light from the surface of samples immersed in liquid was collected and transfiered to spectroscope (consists of grating to analyze the light and CCD array to convert the incident light electrical information) by optical fiber, which was set at angle of about 45 degree off the laser beam axis to avoid splashing, and transfer by optical fiber to the entrance slit of the spectrometer as shown in Figure- 1. The experimental system detail can be seen elsewhere [12].

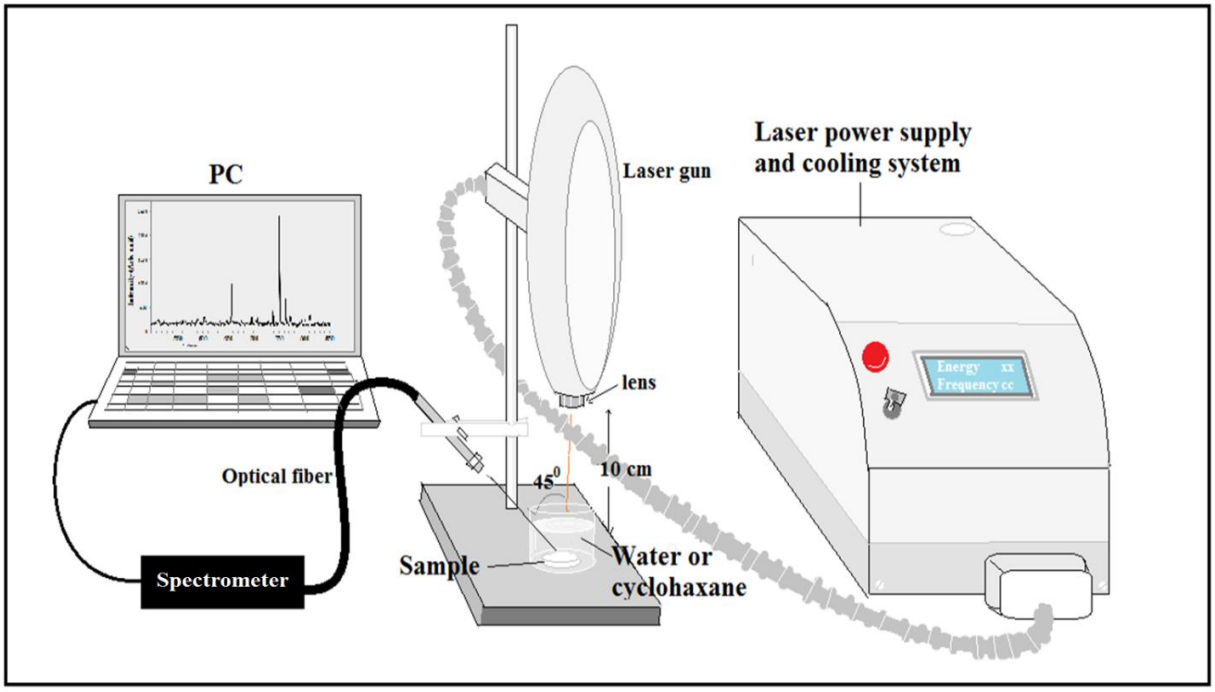

Figure 1- Schematic of LIPS experimental system.

The water consist of Ag:Ni Nanoparticles were analyze by UV-Visible SP-8001 spectrophotometer, work in the wavelength range (190-1100) nm. Then the particles deposited on glass substrate by drop casting technique (solution containing metal nanoparticles is dropped on an a horizontal glass substrate and take them to dry at room temperature) then characterized thin films morphology by AFM and XRD (Shimadzu XRD 6000 Cu target (Kα) with wave length λ= 1.5405 Å) to study the effect of laser energy on produced particles.

The x-ray diffraction peaks broadening is a standard phenomenon to improve the formation of nanoparticles, where the crystalline size estimated by Scherrer equation formula[13].

$$G.S = \frac{0.9\,\lambda}{FWHM\,.\cos(\theta)} \quad (3)$$

where λ is the used x-ray wavelength, FWHM is full width at half maximum (in radians) and θ is diffraction angle.

Results and Discussion

Figure-2 displays the emission spectra for laser induced on Ag:Ni surface with different laser energies (300, 400, 500, 600, 700 and 800) mJ in distilled water using 1064 nm laser. This figure displays that the dominant identified peaks corresponding to silver ionic lines (Ag II) and some of atomic lines for silver and nickel (Ag I, Ni I). The emission spectrum intensity increase with increasing laser energy.

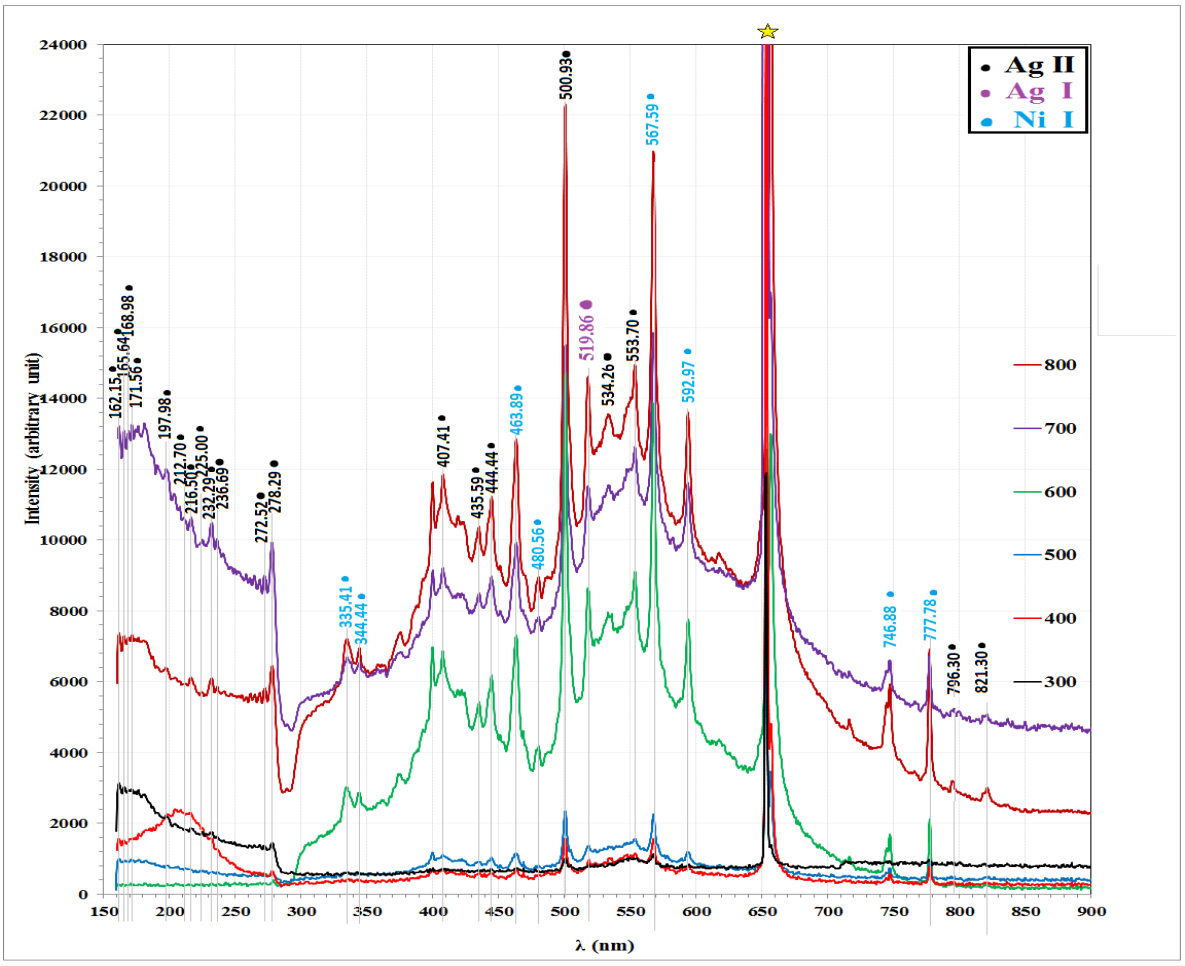

Figure 2- Light emission spectra induced by 1064 nm laser, with different laser energies for Ag:Ni alloy in distilled water.

The value of electron temperature (T_e) is obtained from the Boltzmann plot, as shown in Figure-3 depending on equation (1), from the analysis of nine recorded (Ag II) lines for plasma induced on Ag:Ni alloy in distilled water at different laser energies. The values of T_e were estimated from the inverse of the slope of a linear best fit for the result values. The fitting equations and the average relative standard deviation value R^2 were shown in the figure for all fitting lines. The ideal value values of R^2 is 1.

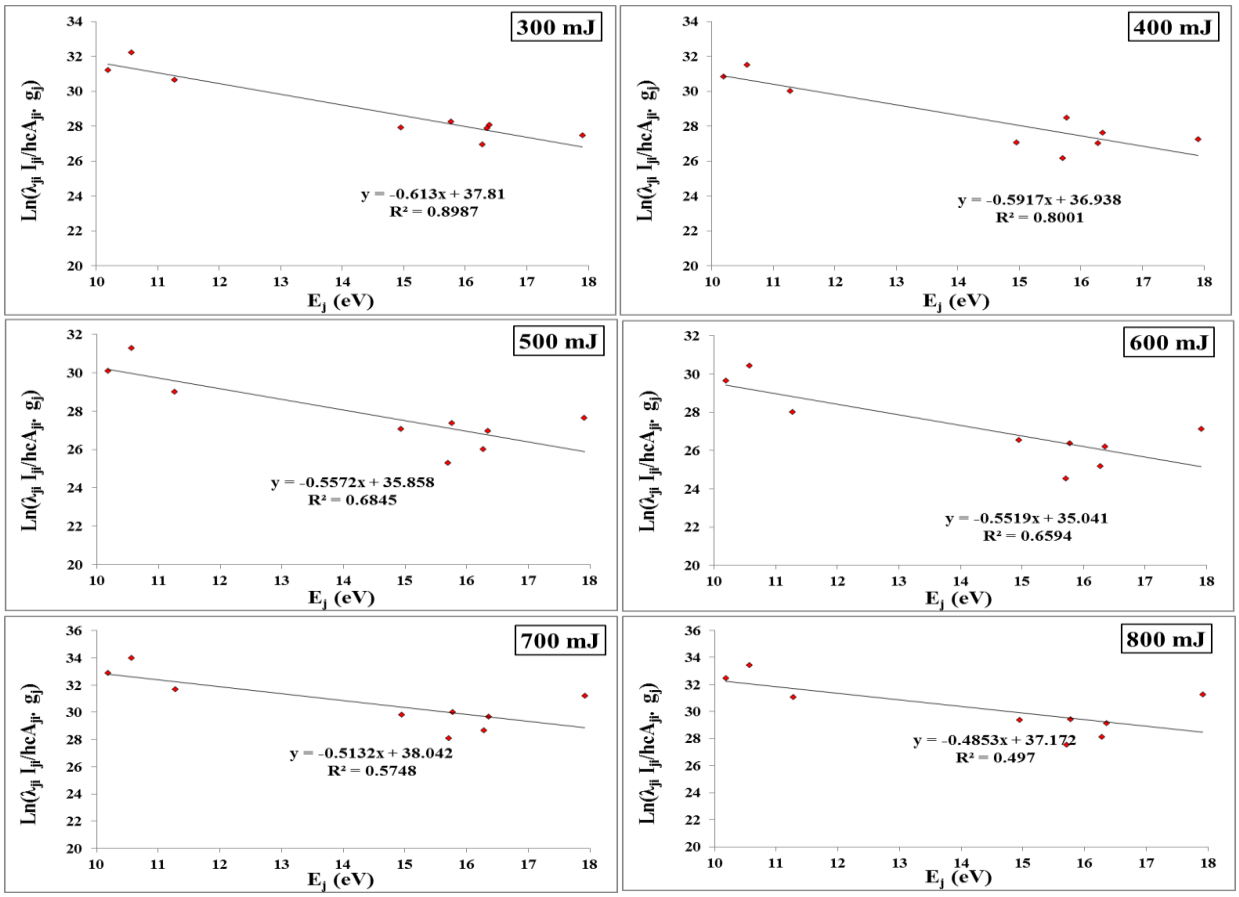

Figure 3- Boltzmann plot made from the analysis of nine Ag II lines for Ag:Ni alloy in distilled water using 1064 nm laser, with different laser energies.

Table-1 shows the experimental calculated values of electron temperature (T_e), electron density (n_e), Debye length (λ_D) , plasma frequency (f_p) and Debye number (N_D) at different laser energies. All calculated plasma parameters were satisfied the plasma criteria. This This table indicate that the electron temperature with increasing laser energy from 300 to 800 mJ as a result of increasing the energy gained to electrons from laser. The increment in mean electron energy cause to increase the probability of ionization collision hence increasing the electron density. Plasma frequency mainly depend on $n_e^{1/2}$, thus it have the same behavior. While λ_D depend on $(T_e/n_e)^{1/2}$ as a result on clearly increasing n_e while slightly increasing in T_e. N_D depend on $(T_e^{3/2} / n_e^{1/2})$ thus it increase then decrease with laser energy.

Table 1- plasma parameters calculated from spectroscopy lines for Ag:Ni alloy in distilled water using 1064 nm laser, with different laser energies.

Laser energy	T_e (eV)	$n_{e*10}{}^{15}$ (cm^{-3})	f_p (Hz) *10^{11}	λ_D (cm)	N_D *10^4
300	1.631	1.39	3.35	0.00025	9.602
400	1.690	1.38	3.33	0.00026	10.057
500	1.795	1.60	3.59	0.00025	10.201
600	1.812	1.75	3.76	0.00024	9.895
700	1.949	2.03	4.04	0.00023	10.261
800	2.060	2.25	4.26	0.00022	10.584

Figure-4 displays the photo for Ag:Ni pellet before and after bombarding with laser. This figure shows the effect of laser on sample surfaces.

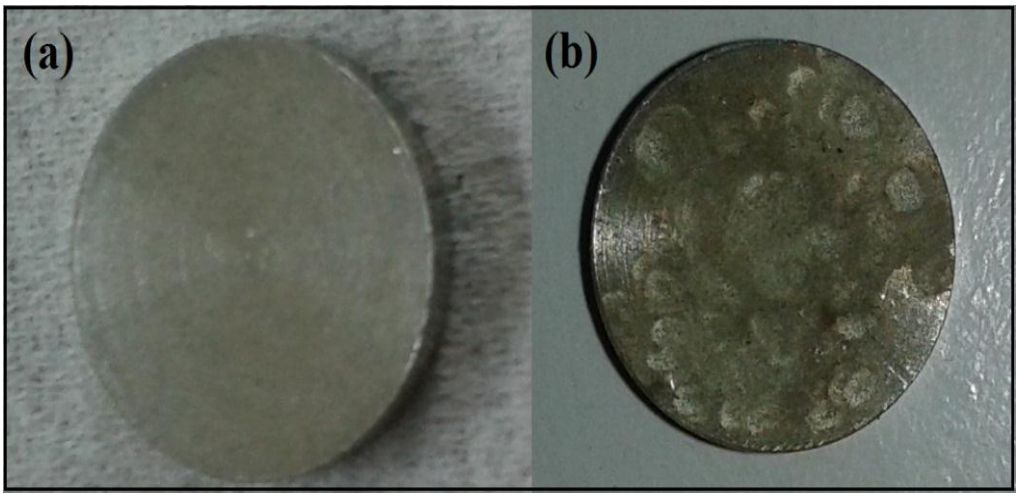

Figure 4- Ag:Ni pellet (a) before and (b) after bombarding with laser

Figure-5 displays the photo for distilled water samples contained Ag:Ni Nano particles. The color change from light to dark off-white with increasing laser energy caused as a result of changing Ag:Ni Nano particle size and the particle concentration in water. The sample with 300 mJ contain small amount of nanoparticles that cannot be deposited and characterized by XRD, AFM and UV visible absorbance.

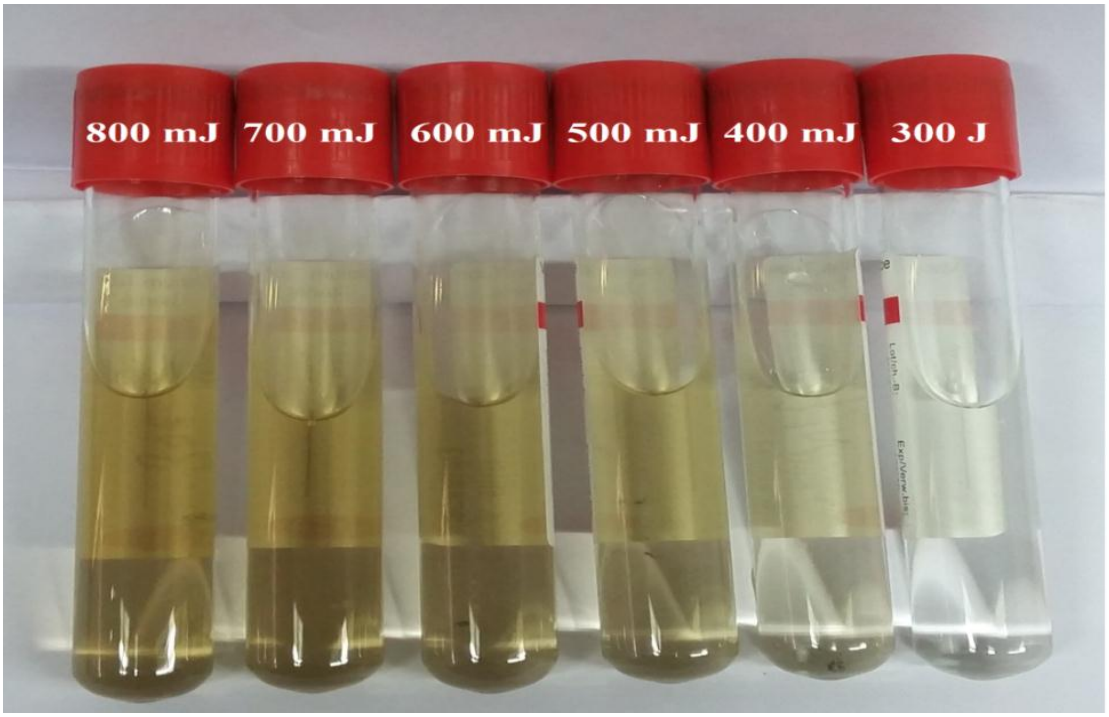

Figure 5- Water contain Ag:Ni nanoparticles produced by pulse laser with different power.

Figure-6 illustrates AFM Images and its granulation distribution for Ag:Ni particles samples deposited on glass slides produced by laser with different energies. This figure shows that the particle diameter decrease with increasing laser energy. Table- 2 , shows the variation of particle size with laser energy, where the particle size decrease from 97.13 nm to 71.20 nm with increasing pulse laser energy from 400 to 800 mJ as a result high expansion of plasma plume.

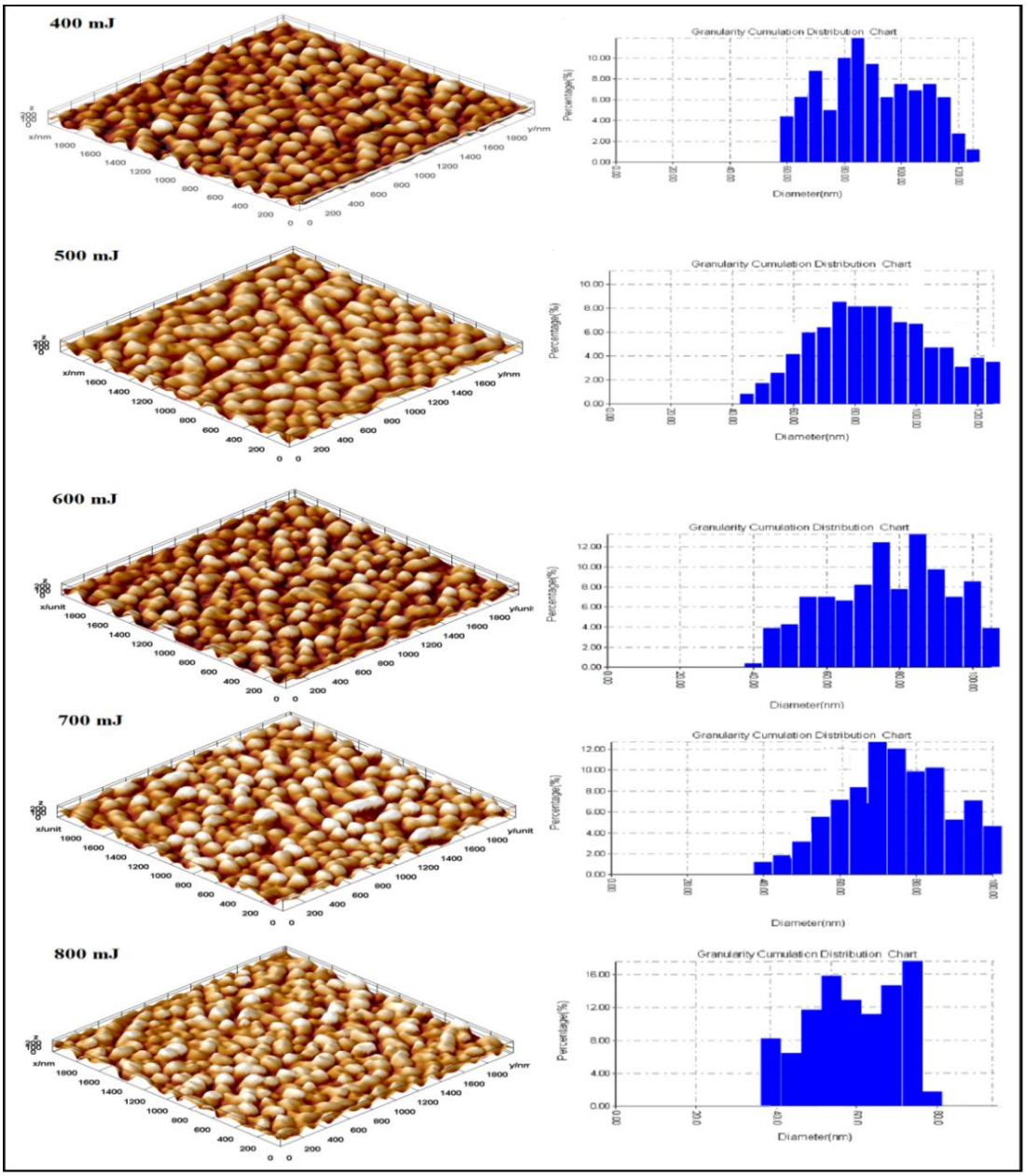

Figure 6- AFM image and the granulation distribution for Ag:Ni particles samples produced by laser with different energies.

Table 2-Average diameter and root mean square roughness for Ag:Ni particles samples produced by laser with different energies

Laser energy (mJ)	Average diameter (nm)	RMS roughness (nm)
400	97.13	1.24
500	85.03	0.620
600	80.26	0.573
700	78.08	1.850
800	71.20	0.750

Figure-7 displays X- ray diffraction for Ag:Ni particles samples on glass substrate. There are four peaks located at 2θ about 37.79, 43.90, 63.80 and 76.57 ^{0} corresponding to (111), (200), (220) and (311) directions respectively for cubic Ag crystals. It can be seen that the full width of half maximum for observed peaks increase with increasing laser energy which indicate on decreasing the crystalline size from about 15.5 nm to 9 nm with increasing laser energy from 400 to 800 nm. Table-3 shows all peaks observed in XRD and a comparison with standard peaks.

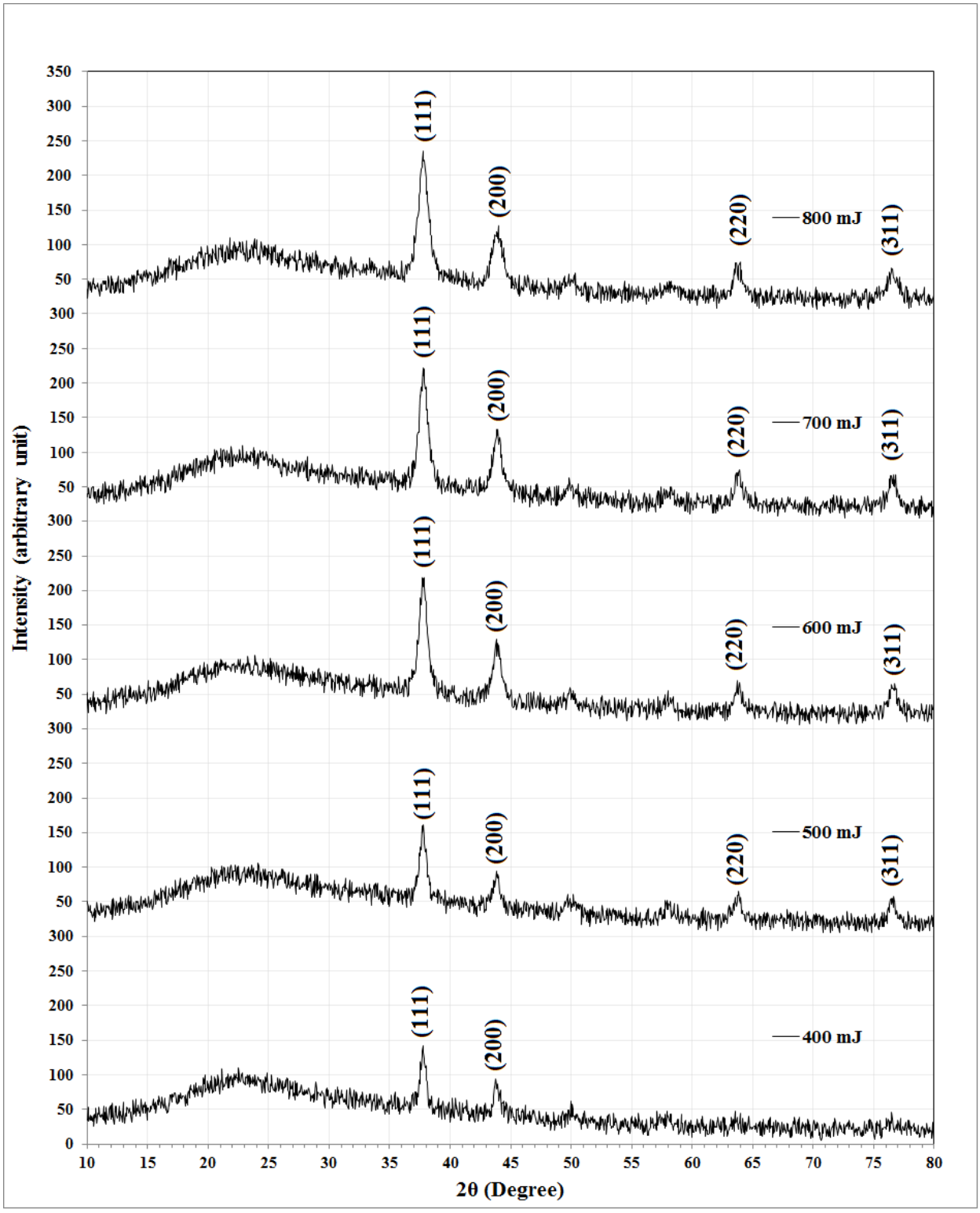

Figure7- XRD patterns for Ag:Ni particles samples produced by laser with different energies.

Table 3- Comparison between experimental and standard XRD peak and calculated crystalline size.

Laser energy (mJ)	2θ (Deg.)	FWHM (Deg.)	d_{hkl} Exp.(Å)	G.S (nm)	hkl	d_{hkl} Std. (Å)	Phase	Card No.
400	37.7449	0.5420	2.3814	15.5	(110)	2.3821	(111)	96-901-3049
	43.8607	0.5487	2.0625	15.6	(101)	2.0630	(200)	96-901-3049
500	37.7561	0.6340	2.3807	13.2	(220)	2.3821	(111)	96-901-3049
	43.8719	0.6418	2.0620	13.3	(130)	2.0630	(200)	96-901-3049
	63.7682	0.6497	1.4583	14.4	(301)	1.4588	(220)	96-901-3049
	76.5397	0.6577	1.2437	15.4	(321)	1.2440	(311)	96-901-3049
600	37.7673	0.7920	2.3801	10.6	(110)	2.3821	(111)	96-901-3049
	43.8831	0.8017	2.0615	10.7	(101)	2.0630	(200)	96-901-3049
	63.7794	0.8116	1.4581	11.5	(200)	1.4588	(220)	96-901-3049
	76.5509	0.8216	1.2435	12.3	(211)	1.2440	(311)	96-901-3049
700	37.7785	0.8320	2.3794	10.1	(220)	2.3821	(111)	96-901-3049
	43.8943	0.8422	2.0610	10.2	(130)	2.0630	(200)	96-901-3049
	63.7906	0.8526	1.4579	11.0	(112)	1.4588	(220)	96-901-3049
	76.5621	0.8631	1.2434	11.7	(301)	1.2440	(311)	96-901-3049
800	37.7897	0.9510	2.3787	8.8	(202)	2.3821	(111)	96-901-3049
	43.9055	0.9627	2.0605	8.9	(321)	2.0630	(200)	96-901-3049
	63.8018	0.9745	1.4577	9.6	(110)	1.4588	(220)	96-901-3049
	76.5733	0.9865	1.2432	10.3	(101)	1.2440	(311)	96-901-3049

Figure-8 shows the absorption spectrum for Ag:Ni nanoparticles in distilled water. In general the absorbance increase at all range with increasing laser energy as a result of increasing number of produced particles in water. Peaks appear in all samples around 400 nm caused from plasmon effect, as a result of interaction of incident light with electrons surrounded by particles walls. It is well known that Ag nanoparticles have plasmon absorption bands at about 400 nm [14]. The absorption maximum moves from 410 to 395 nm when laser energy increase (from 400 to 800) mJ, i.e. with decreasing particle diameter from 97 to 71 nm this result is in agreement with researches have reported in Nano range diameter particle size effects on plasmon absorption peaks, perhaps slightly changing resonance effects[15].

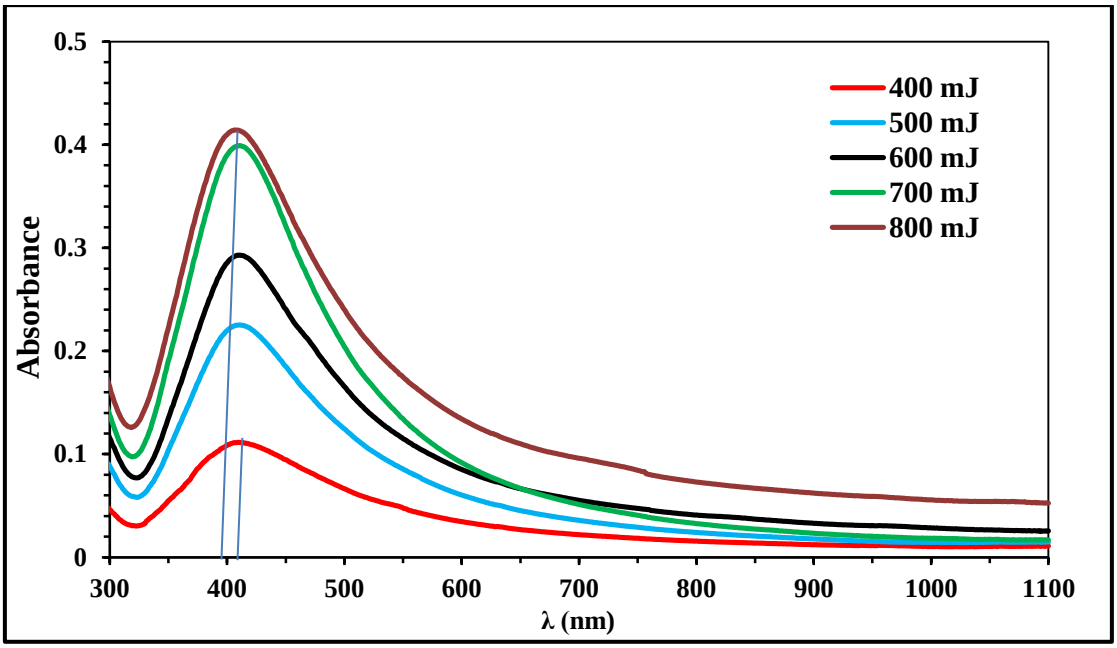

Figure 8- Absorbance spectrum of Ag:Ni Nano particles produced by pulls laser with different power on Ag:Ni target in distilled water.

Conclusions

Increasing laser energy leads to increase both the electron temperature and electron density caused by increasing energy gained to electrons in confined plasma in water which lead to increasing the ionization collision rate and create more electrons, which cause highly expansion in plasma plume leads to effect on produced nanoparticles.

The study of laser energy effect on size of produced Ag:Ni nanoparticles confirmed that changing of laser energy is a good tool to control the nanoparticles size where the particle size decrease with increasing laser energy from 400 to 800 mJ.

The XRD for produced Nano particles shows that the crystallinety of Ag:Ni nanoparticles increase and the crystalline size decrease with increasing laser peaks energy from 400 to 800 mJ. Decreasing the particle size effect on plasmon peak position in absorption spectra, where the peak experience a blue shift with reducing particles size.

References

1. Daniel, L. F. and Colby. A. F. **2002**. *Metal Nano Particles Synthesis, Characterization and Applications*. United state, New York: Marcel Dekker Inc., p147.
2. Huang, X., El-Sayed, I., Qian,W. and El-Sayed, M.. **2006.** Cancer cell imaging and photothermal therapy in the near-infrared region by using gold nanorods. *J. Am. Chem. Soc.*, **128**(6): 2115–2120.
3. Chan, G. H., Zhao, J. E. Hicks, M. G. Schatz, C. and Van Duyne, R. P. **2007.** Plasmonic Properties of Copper Nanoparticles Fabricated by Nanosphere Lithography. *NANO Lett. Plasmonic*, **7(**7): 1947–1952.
4. Wankhede, P. Sharma, P. K. and Jha, A. K. **2013.** Synthesis of Copper Nanoparticles through Wire Explosion Route. *J. Eng. Res. Appl.*, **3(**6): 1664–1669.
5. Koao, L. F. Dejene, F. B. and Swart, H. C. **2014.** Synthesis of PbS Nanostructures by Chemical Bath Deposition Method. *Int. J. Electrochem. Sci.*, **9:** 1747–1757.
6. Chen, G. X. Hong, M. H. and Chong, T. C. **2004.** Preparation of carbon nanoparticles with strong optical limiting properties by laser ablation in water. *J. Appl. Phys.*, **95**(3): 1455–1459.
7. Chamorro, J. Uzuriaga, J. and Riascos, H. **2012.** Laser induced aluminiun plasma analysis by optical emission spectroscopy in a nitrogen background gas. *J. Phys.*, **370:** 12051.
8. Unnikrishnan, V., Alti, K., Kartha, V., Santhosh, C. Gupta, G. and Suri, B. **2010.** Measurements of plasma temperature and electron density in laser-induced copper plasma by time-resolved spectroscopy of neutral atom and ion emissions. *Pramana - J. Phys.*, **74**(6): 983–993.
9. Hamed, S. S. **2005.** Spectroscopic Determination of Excitation Premixed Laminar Flame. *Egypt J.*

Solids, **28**(2): 349–357.

10. Dinklage, A., Klinger, T., Marx, G. and Schweikhard, L. **2005**. *Plasma Physics, Confinement, Transport and Collective Effects.* Series: Lecture Notes in Physics, Springer-Verlag, Berlin, Heidelberg Vol. 670.

11. Dupas, C. **2007.** *Nanoscience.* Belin, France: Springer-Verlag Berlin Heidelberg, p. 620.

12. Ali A-K. Hussain and Ahmed Abd Al-Razzaq .**2016.** Plasma characteristics of Ag:Al alloy using fundamental and second harmonic frequencies of Nd:YAG Laser. *Iraqi J. Appl. Phys.*, p. 765.

13. Yang, P. **2003.** *The Chemistry of Nano Structured Materials*. Printed in Singapore.: World Scientific Publishing Co. Pte. Ltd., p. 362.

14. Alqudami, A. and Annapoorni, S. **2008.** Ag – Au alloy nanoparticles prepared by electro-exploding wire technique. *J. Nanopart Res.*, **10**: 1027–1036.

15. Tarasenko, N. V., Burakov,V. S. and Butsen, A. V. **2007.** Laser Ablation Plasmas In Liquids For Fabrication of Nanosize Particles. *Publ. Astron. Obs. Belgrade,* **82:** 201–211.